Imatinib (STI571)-Mediated Changes in Glucose Metabolism in Human Leukemia BCR-ABL–Positive Cells

Sven Gottschalk,[1] Nora Anderson,[2] Carsten Hainz,[1] S. Gail Eckhardt,[3] and Natalie J. Serkova[1,2]

[1]Department of Biology/Chemistry, University of Bremen, Bremen, Germany; and [2]Department of Anesthesiology and [3]Division of Medical Oncology, University of Colorado Health Sciences Center, Denver, Colorado

ABSTRACT

The therapeutic efficacy of imatinib mesylate (Gleevec) is based on its specific inhibition of the BCR-ABL oncogene protein, a widely expressed tyrosine kinase in chronic myelogenous leukemia (CML) cells. The goal of this study was to evaluate glucose metabolism in BCR-ABL–positive cells that are sensitive to imatinib exposure. Two human BCR-ABL–positive cell lines (CML-T1 and K562) and one BCR-ABL–negative cell line (HC-1) were incubated with different imatinib concentrations for 96 hours. Magnetic resonance spectroscopy on cell acid extracts was performed to evaluate [1-^{13}C]glucose metabolism, energy state, and changes in endogenous metabolites after incubation with imatinib. Imatinib induced a concentration-dependent inhibition of cell proliferation in CML-T1 (IC_{50}, 0.69 ± 0.06 μmol/L) and K562 cells (IC_{50}, 0.47 ± 0.04 μmol/L), but not in HC-1 cells. There were no metabolic changes in imatinib-treated HC-1 cells. In BCR-ABL–positive cells, the relevant therapeutic concentrations of imatinib (0.1–1.0 μmol/L) decreased glucose uptake from the media by suppressing glycolitic cell activity (C3-lactate at 0.25 mmol/L, 65% for K562 and 77% for CML-T1 *versus* control). Additionally, the activity of the mitochondrial Krebs cycle was increased (C4-glutamate at 0.25 μmol/L, 147% for K562 and 170% for CML-T1). The improvement in mitochondrial glucose metabolism resulted in an increased energy state (nucleoside triphosphate/nucleoside diphosphate at 0.25 μmol/L, 130% for K562 and 125% for CML-T1). Apoptosis was observed at higher concentrations. Unlike standard chemotherapeutics, imatinib, without cytocidal activity, reverses the Warburg effect in BCR-ABL–positive cells by switching from glycolysis to mitochondrial glucose metabolism, resulting in decreased glucose uptake and higher energy state.

INTRODUCTION

Chronic myelogenous leukemia (CML) accounts for approximately 20% of newly diagnosed cases of leukemia in adults. About 20% to 30% of patients with CML will die within 2 years of the diagnosis, and about 25% die each year after that. The standard treatment with busulfan and interferon palliates the disease but does not prolong life (1, 2). CML is one of the most carefully studied and best understood cancers in humans: it is triggered by a translocation of chromosome 22 onto chromosome 9 in leukocytes (3). This translocation, known now as the Philadelphia chromosome t(9;22)(q34:q22), creates the fused oncogene BCR-ABL that is expressed as a tyrosine kinase fusion protein (4, 5). Tyrosine kinases play a key role in tumor development by promoting cell growth through phosphorylation of signaling proteins, *e.g.*, ras-GTPase-activating protein for the BCR-ABL tyrosine kinase (5). Understanding the molecular mechanism responsible for the etiology of CML allowed for the development of a specific signal transduction inhibitor now known as imatinib.

Imatinib (Gleevec, formerly STI571) is designed chemically as 4-[(4-methyl-1-piperazinyl)methyl]-*N*-[4-methyl-3[[4-(3-pyridinyl)-2-pyrimidinyl]aminophenyl]benzamide methanesulfonate) (molecular weight of 589.7). Imatinib functions through competitive inhibition at the ATP-binding site of the BCR-ABL enzyme, which leads to the inhibition of tyrosine phosphorylation of proteins involved in BCR-ABL signal transduction (6). In preclinical studies, the inhibition of cell proliferation (IC_{50}, approximately 0.4 μmol/L) of BCR-ABL–positive cells was followed by apoptosis (6, 7). Imatinib is also an inhibitor of the receptor tyrosine kinase for platelet-derived growth factor and stem cell factor (8). Imatinib inhibits proliferation and induces apoptosis in gastrointestinal stromal tumor cells, which express an activating c-KIT mutation (9, 10). Molecular targeting of signal transduction molecules by imatinib has greatly improved the treatment of chronic phase and blast crisis in CML. Results from phase I and II studies have demonstrated that the IC_{50} for BCR-ABL tyrosine kinase inhibition in patients leukocytes was 0.25 μmol/L (11, 12). The major concern regarding imatinib treatment is, to date, the development of drug resistance in CML patients (12, 13). Although correlations between molecular effects of imatinib and clinical efficacy have been well established, there is little information regarding the changes in cell metabolism in CML cells during exposure to imatinib. However, it has been suggested that the control of glucose-substrate flux is an important mechanism of the antiproliferative action of imatinib because BCR-ABL–positive cells, like most malignant cells, express the high-affinity GLUT-1 glucose transporter and demonstrate increased glucose uptake (14). Also, it has been shown in clinical positron emis-

Received 1/7/04; revised 3/16/04; accepted 3/22/04.
The costs of publication of this article were defrayed in part by the payment of page charges. This article must therefore be hereby marked *advertisement* in accordance with 18 U.S.C. Section 1734 solely to indicate this fact.

Requests for reprints: Natalie Serkova, Biomedical MRI/MRS Facility, Department of Anesthesiology, 4800 East Ninth Avenue, UH-2122, Box 113, Denver, CO 80262. Phone: 303-315-1878; Fax: 303-315-1858; E-mail: Natalie.Serkova@uchsc.edu.

sion tomography (PET) scans that glucose uptake is highly elevated in patients with imatinib-resistant c-KIT–positive malignancies (15). Hence, the evaluation of the metabolic response of leukemia cells to imatinib treatment may yield important biological markers of imatinib sensitivity in CML and other tumors.

Magnetic resonance spectroscopy (MRS) has been used extensively in the last decade to investigate cancer metabolism (16–18). After tumor cell incubation with [^{13}C]glucose, ^{13}C MRS detects changes in glucose utilization and metabolism in tumor cells and is able to distinguish mitochondrial from cytosolic glycolitic pathways. ^{31}P MRS allows for assessment of energy state and phospholipid metabolism, both of which are involved in tumor proliferation and response to therapy. Finally, ^{1}H MRS yields well-resolved peaks from large numbers of endogenous metabolites and allows for absolute quantification of lipids, glucose, lactate, major amino acids, and osmoregulators, among others. Because signals from all detectable metabolites are observed simultaneously, MRS is a powerful technique for investigating a broad spectrum of treatment-associated cellular metabolic changes in cancer cells.

In this series of experiments, we hypothesized that the metabolic response of human BCR-ABL–positive cells to imatinib would reflect changes in glucose metabolism and correlate with inhibition of signal transduction and induction of cell death. Thus, the aim of the present study was to assess the dose-dependent metabolic and cellular response of human leukemia cells (BCR-ABL–positive *versus*–negative cells) to imatinib treatment.

MATERIALS AND METHODS

Cell Cultures and Imatinib Treatment. Two human BCR-ABL–positive cell lines (CML-T1 and K562) and one BCR-ABL–negative cell line (HC-1) were purchased from the German Collection of Microorganisms and Cell Cultures (Deutsche Sammlung von Mikroorganismen und Zellkulturen, Braunschweig, Germany). All cells were grown in RPMI 1640 culture medium containing 10% (CML-T1 and K562) or 20% (HC-1) fetal bovine serum as recommended by the Deutsche Sammlung von Mikroorganismen und Zellkulturen. Cell density was maintained at approximately 0.3×10^6 cells per milliliter of medium in 240-mL culture flasks. The cells were incubated at 37°C with 95% air/5% CO_2 (v/v) and subcultured at a 1:4 dilution every 96 hours. Imatinib was kindly provided by Novartis Pharma AG (Basel, Switzerland). Various concentrations of imatinib (0.05, 0.1, 0.25, 0.5, 1, 2, 5, and 10 μmol/L) were added to the incubation media for up to 96 hours. Every second day, the total volume of incubation media was doubled by adding fresh medium to maintain the correct cell density and nutrition balance. Cell proliferation and viability were checked every 24 hours by cell counting using a hemocytometer and trypan blue exclusion. For MRS experiments, the following imatinib concentrations were tested: 0, 0.1, 0.25, 1.0, and 2.5 μmol/L. The cells were then incubated with 5 mmol/L [1-^{13}C]glucose for the last 4 hours of treatment before perchloric acid (PCA) extraction.

Cell Extraction for Magnetic Resonance Spectroscopy. All cell extractions were performed using a previously published PCA extraction protocol (19). In brief, for each extract, approximately 1×10^8 cells were pooled together. The cells were washed, centrifuged (5 minutes at $400 \times g$), weighed, and frozen in liquid nitrogen. The cells were then extracted with 4 mL of ice-cold PCA (12%). The samples were centrifuged (15 minutes at $1{,}300 \times g$), and the aqueous phase was removed and neutralized using KOH. The samples were centrifuged again and lyophilized overnight. The incubation media were also collected immediately after experiments, and the media were lyophilized overnight. The lyophilized PCA cell extracts were redissolved in 0.45 mL of deuterium oxide, the lyophilized media were redissolved in 1 mL of deuterium oxide. After centrifugation, the supernatants were analyzed by MRS.

Magnetic Resonance Spectroscopy Experiments. All high-resolution MRS experiments were performed in a 360 MHz Bruker Avance NMR spectrometer (Bruker, Karlsruhe, Germany) as reported previously (19, 20). A 5-mm QNP probe head was used for all nuclei. For proton MRS, the operating frequency was 360 MHz, and a standard water presaturation pulse program was used for water suppression. Trimethylsilyl propionic-2,2,3,3,-d_4 acid (TSP) (TSP, 0.5 mmol/L for cell PCA extracts and 1.2 mmol/L for media) was used as an external standard for metabolite quantification from fully relaxed ^{1}H magnetic resonance (MR) spectra. ^{1}H chemical shifts were referenced to TSP at 0 ppm. ^{13}C MR spectra with proton decoupling were subsequently recorded after ^{1}H MRS. The C3 peak of lactate at 21 ppm was used as chemical shift reference in ^{13}C MRS. Before ^{31}P MR spectra were recorded, EDTA (100 mmol/L) was added to each PCA extract to complex divalent cations. Methylene diphosphoric acid (3 mmol/L) was used as an external standard for metabolite quantification in ^{31}P MRS. The chemical shift of methylene diphosphoric acid at 18 ppm was also used as a chemical shift reference. The data were processed using the WINNMR program (Bruker).

DNA Fragment Assay. Electrophoresis (1.75% agarose) of DNA extracts of treated cells and ethidium bromide staining were used to assess DNA fragmentation as a criterion for apoptosis (21). After centrifugation (5 minutes at $400 \times g$), the cells were incubated with 0.1 mg/mL RNase A at 37°C for 40 minutes in lysate buffer [10 mmol/L Tris-HCl, 10 mmol/L EDTA, and 0.6% SDS (pH 8.0)]. Protein content was precipitated with 5 mol/L NaCl (60 minutes, 4°C), and the DNA was purified from the supernatant by standard chloroform-phenol extraction. Isopropanol was added, and the mixture was stored overnight at −20°C. After centrifugation (15 minutes at $13{,}500 \times$ g, 4°C), the DNA pellet was resuspended in Tris-buffer [10 mmol/L Tris-HCl and 1 mmol/L EDTA (pH 8.0)]. The samples were subjected to electrophoresis on 1.75% agarose gel, and the DNA was stained with ethidium bromide. Ultraviolet spectroscopy at 302 nm was used to report results.

Western Blot Analysis on BCR/ABL Activity. Tyrosine kinase activity was assessed by Western blot analysis. Protein lysates were electrophoresed on 7% SDS-PAGE gels and blotted onto polyvinylidene difluoride membranes by semi-dry electrophoretic transfer (5, 6). The gel was then stained with Coomassie Blue to document equal protein loading. The membrane was blocked with 3% dry milk and 0.1% Tween 20 in PBS and incubated with primary antibodies (PY-99 anti-phosphotyrosine, anti-Abl Ab-3, and anti-Bcr; Santa Cruz Biotechnology, Santa Cruz, CA). The filters were washed and incubated with

horseradish peroxidase-conjugated donkey antirabbit antibodies, and relative quantities of proteins were determined.

Statistical Analysis. All results were calculated as means ± SD for each series of experiments ($n = 4$ for each experimental group). The results from the treated cells were compared with the untreated controls using unpaired Student's *t* test (TTest procedure, SPSS 11.5; SPSS, Chicago, IL).

RESULTS

Cell Proliferation and Viability. After 96 hours, incubation with imatinib inhibited cell proliferation of BCR-ABL–positive cell lines CML-T1 (IC_{50}, 0.69 ± 0.06 μmol/L) and K562 (IC_{50}, 0.47 ± 0.04 μmol/L), but had no effect on the cell growth of BCR-ABL–negative HC-1 cells (Fig. 1). Proliferation of BCR-ABL–positive cells was significantly inhibited even at low imatinib concentrations (starting at 0.1 μmol/L; $P = 0.04$), whereas at higher imatinib concentrations, dead cells were identified by trypan blue exclusion. Using ethidium bromide staining of DNA extracts, the K562 cell line appeared more sensitive to apoptosis by imatinib than did the CML-T1 cells. For example, DNA fragmentation into oligonucleosome-length fragments was observed at concentrations of 1 μmol/L in K562 cells (Fig. 2), whereas concentrations of 5 to 10 μmol/L were required to induce similar effects in CML-T1 cells.

Inhibition of cell proliferation in BCR-ABL cells was accompanied by inhibition of tyrosine phosphorylation. Even at the lowest concentrations (starting at 0.1 μmol/L for K562 and 0.25 μmol/L for CML-T1), imatinib almost completely inhibited BCR-ABL tyrosine kinase activity, as early as 2 hours after exposure.

Glucose Uptake. To assess the changes in glucose uptake and metabolism, the CML-T1, K562, and HC-1 cells were incubated with [1-^{13}C]glucose for the last 4 hours of imatinib treatment. Lyophilized media were used to calculate the concentrations of extracellular glucose (Glc_e) *versus* intracellular glucose (Glc_i) in cell extracts as a criterion for glucose uptake (Glc_e/Glc_i; normalized to the cell mass). All three cell lines demonstrated low Glc_i concentrations, due in part to the high rate of glucose utilization through glycolysis (see below). Extracellular and intracellular concentrations of glucose, as well as their ratios in untreated control cells, are presented in Table 1. Imatinib treatment significantly increased Glc_e in the two BCR-ABL–positive cell lines, which resulted in increased ratios of Glc_e/Glc_i (Fig. 3) and decreased glucose uptake. Conversely, no changes in glucose uptake were observed in the HC-1 cells (Fig. 3).

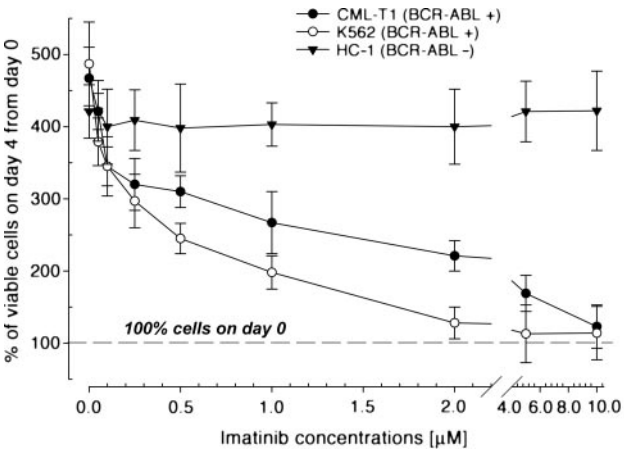

Fig. 1 Cell proliferation in human CML cells 96 hours after incubation with imatinib. The number of untreated cells on day 0 before imatinib exposure served as 100% of viable cells.

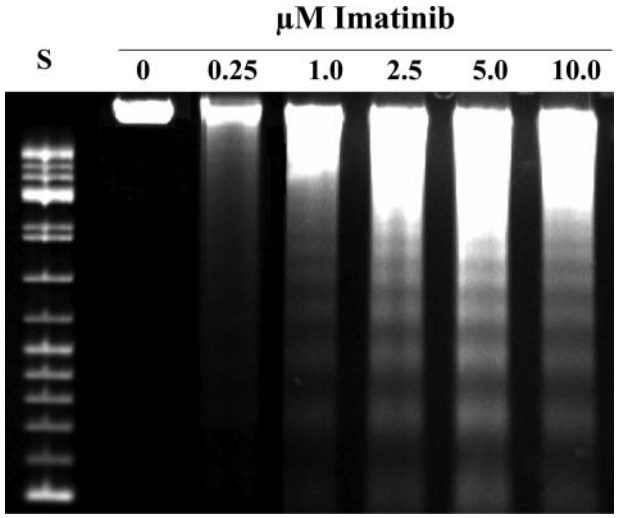

Fig. 2 Induction of apoptosis in human K562 BCR-ABL–positive cells by imatinib. The first ladder-like pattern of DNA fragmentation into oligonucleosome-length fragments was observed in K562 cells by 1 μmol/L imatinib (and in CML-T1 cells by 5 μmol/L imatinib; data not shown).

Table 1 Glc_e and Glc_i concentrations and Glc_e/Glc_i ratios for untreated K562, CML-T1, and HC-1 leukemia cells after 4 hours of incubation with 5 mmol/L [1-^{13}C]glucose

Cell line	Glc_e (μmol/mL)	Glc_i (μmol/g)	Glc_e/Glc_i
K562	3.256 ± 0.471	0.025 ± 0.004	0.41×10^3
CML-T1	3.846 ± 0.285	0.032 ± 0.002	0.38×10^3
HC-1	3.071 ± 0.831	0.012 ± 0.007	0.69×10^3

NOTE. The absolute concentrations of Glc_e were calculated from ^{1}H and ^{13}C MRS of lyophilized media, and the absolute concentrations of Glc_i were calculated from ^{1}H and ^{13}C MRS of cell PCA extracts. Absolute concentrations of glucose are presented as mean ± SD ($n = 4$). The Glc_e/Glc_i ratios were normalized to the cell mass and represent (absolute concentration Glc_e/absolute concentration Glc_i/cell weight).

Glucose Metabolism. The cellular response in both BCR-ABL–positive cells reflected the same metabolic pattern. After 96 hours of imatinib treatment, glucose metabolism was changed from anaerobic glycolysis (lactate production) to the mitochondrial Krebs cycle (Fig. 4*A*). After incubation with 0.25 μmol/L imatinib for 96 hours, C3-lactate metabolized from [1–13C]glucose in the last 4 hours of incubation decreased to 65% ($P = 0.002$) and 77% ($P = 0.03$) of the untreated control in K562 and CML-T1 cells, respectively (Figs. 4*A* and 5*A*). The decreased production of labeled lactate indicated a decreased rate of cytosolic glucolysis in imatinib-treated cells. Concurrently, production of C4-glutamate from [1-^{13}C]glucose

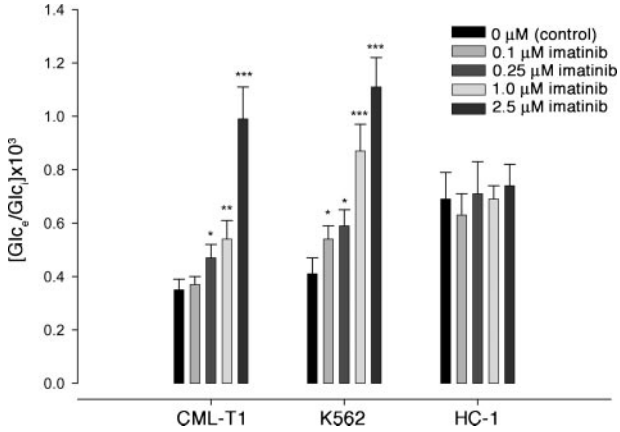

Fig. 3 Changes in the Glc_e/Glc_i ratio normalized to cell masses after 96 hours of imatinib treatment. The ratios were calculated as absolute concentrations of Glc_e/Glc_i/cell weight after 4 hours of incubation with 5 mmol/L [1-^{13}C]glucose. The Clc_e concentrations were calculated from MR spectra of incubation media, and the Glc_i concentrations were calculated from MR spectra of cell PCA extracts ($n = 4$ for each imatinib concentration). Statistical significance as compared with the untreated control was as follows: *, $P < 0.05$; **, $P < 0.01$; and ***, $P < 0.001$ (unpaired TTest; $n = 4$).

(through pyruvate) increased to 147% ($P = 0.009$) in K562 and 170% ($P = 0.001$) in CML-T1 cells (Figs. 4*A* and 5*B*). Glutamate is the major intermediate from the Krebs cycle, and the increased production of labeled glutamate indicated increased utilization of the mitochondrial glucose pathway. Interestingly, activation of the Krebs cycle disappeared at the higher imatinib concentrations (Fig. 5*B*). No changes were observed in glucose metabolism of BCR-ABL–negative HC-1 cells (Fig. 5*A* and *B*).

Energy State after Imatinib Treatment. The increase in mitochondrial glucose metabolism was accompanied by higher energy state in imatinib-treated BCR-ABL–positive cells (Fig. 4*B*). Imatinib treatment (0.1–1.0 μmol/L concentration range) increased absolute concentrations of the high energy phosphate nucleoside triphosphate (NTP) and, subsequently, the cell energy balance [(NTP/nucleoside diphosphate (NDP); Fig. 5*C*]. The energy change increased to 130% ($P = 0.03$) and 125% ($P = 0.02$) of untreated control cells in K562 and CML-T1 cells, respectively. Similar to the lack of changes in mitochondrial glucose metabolism observed above at higher concentrations of imatinib, concentrations of 2.5 μmol/L were not associated with an increase in the energy state (Fig. 5*C*). For example, a decrease in the NTP/NDP ratio to 68% in K562 cells

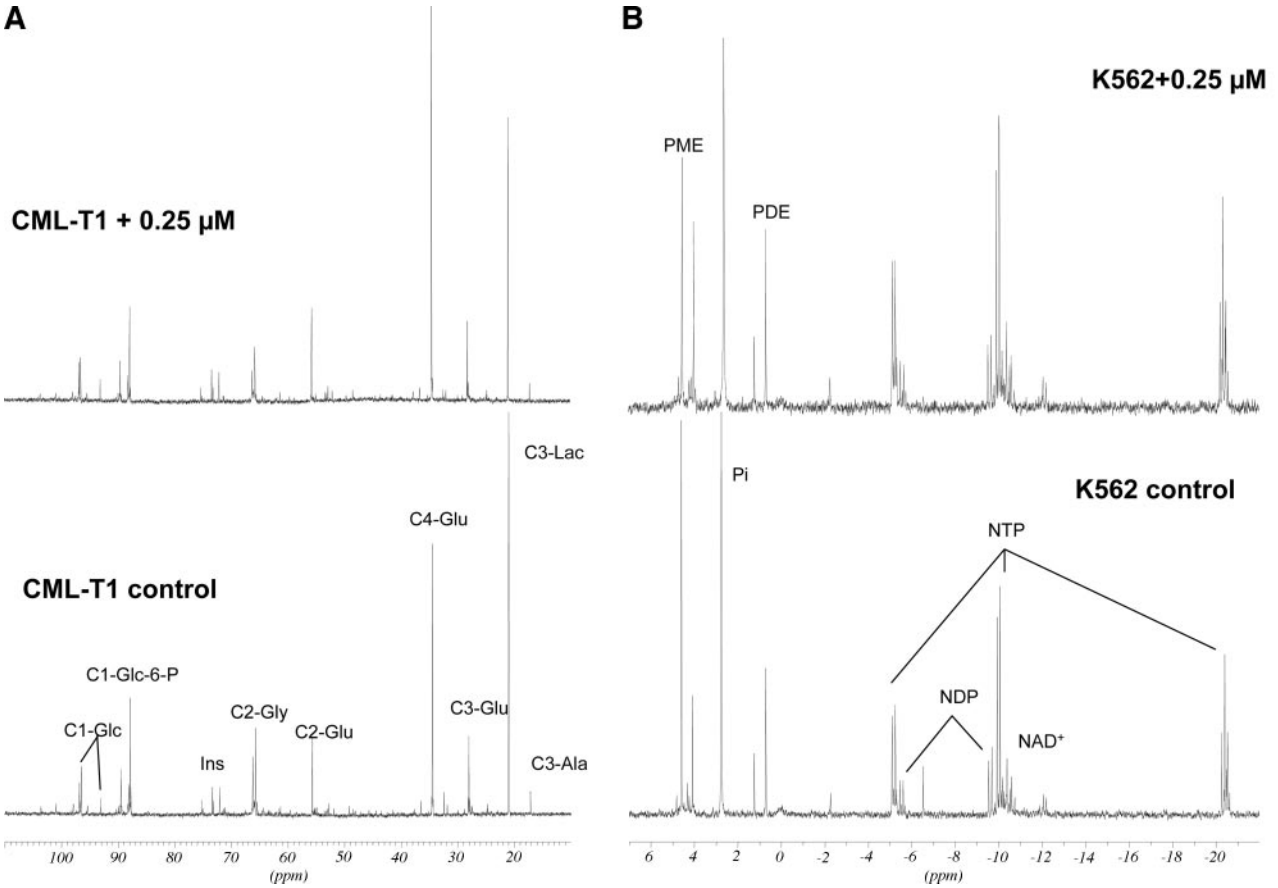

Fig. 4 Representative MR spectra of leukemia cell extracts after 96 hours of incubation with imatinib. *A*, ^{13}C MRS of human CML-T1 cells after addition of 5 mmol/L [1-^{13}C]glucose for 4 hours; *B*, ^{31}P MRS of human K562 cell extracts. *Glc*, glucose; *Glu*, glutamate (C4 labeling from C1-glucose through pyruvate dehydrogenase; C3 and C2 labeling through pyruvate carboxylase); *Lac*, lactate (C3 labeling from C1-glucose through LDH); *PDE*, glycerophosphocholine; *PME*, phosphocholine.

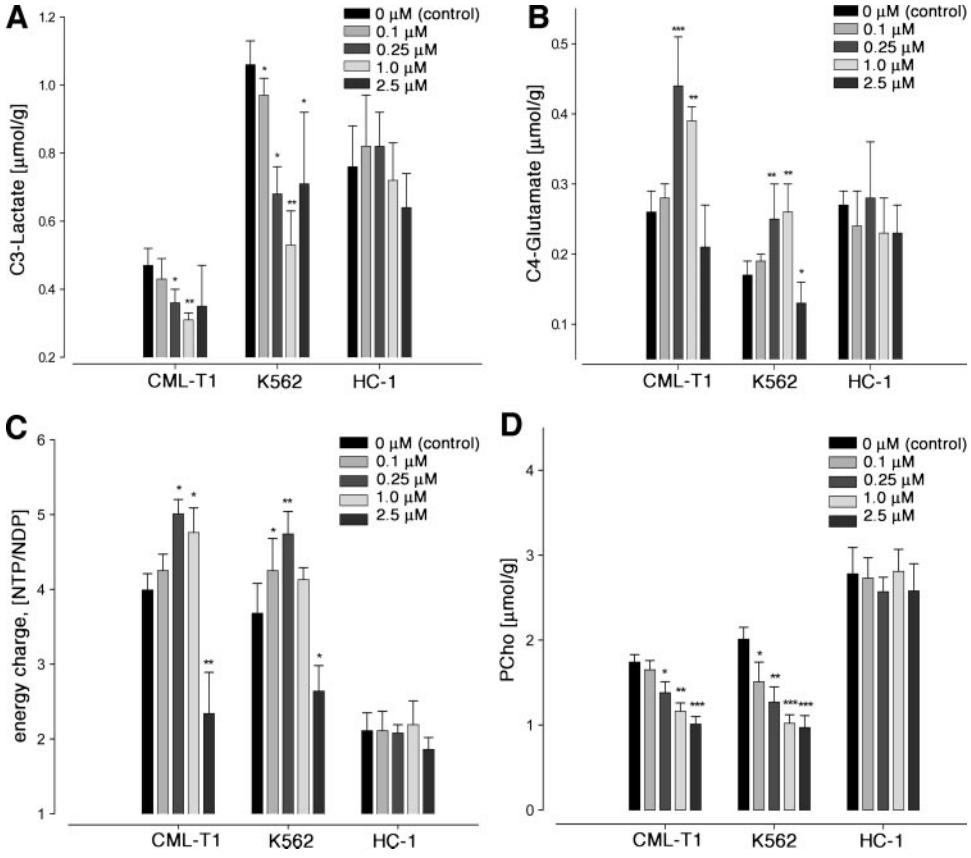

Fig. 5 Changes in C3-lactate (*A*), C4-glutamate (*B*), energy charge (*C*), and phosphocholine (*D*) after 96 hours of incubation with imatinib calculated from ^{13}C- and ^{31}P MRS spectra. The concentrations of ^{13}C-labeled lactate (*A*) and glutamate (*B*) are given as micromole per gram of cell weight based on satellite peaks of [^{13}C]lactate calculated from ^{1}H MRS. *Asterisk* indicates statistically significant difference from the untreated control. *, $P < 0.05$; **, $P < 0.01$; ***, $P < 0.001$ (unpaired TTest; $n = 4$). *PCho*, phosphocholine.

($P = 0.03$) and 59% in CML-T1 cells ($P = 0.01$) of the control cells was observed at the 2.5 μmol/L concentrations of imatinib. Imatinib did not affect the energy metabolism of BCR-ABL–negative HC-1 cells (Fig. 5*C*).

Changes in Phospholipid Metabolism. Another significant difference in the metabolic response of imatinib-treated BCR-ABL–positive cells was a significant decrease in phosphocholine concentrations [phosphomonoesters (PMEs); PME peak on Fig. 4*B*). Imatinib led to a decrease in PME concentrations, observed in K562 cells at the lowest concentration of 0.1 μmol/L. Phosphocholine concentrations calculated from ^{1}H MRS were 1.51 ± 0.23 *versus* 2.01 ± 0.14 μmol/g in untreated K562 cells ($P = 0.04$). Phosphocholine is a precursor of membrane phospholipid (*e.g.*, phospholipid synthesis), and increased presence of phosphocholine is a marker for various cancers with high proliferation rates. For imatinib, the decrease of PME was concentration dependent (Fig. 5*D*) and was accompanied at higher imatinib concentrations with an increase in phosphodiester (PDE) signals (mainly glycerophosphocholine; Fig. 4*B*). Glycerophosphocholine concentrations after 96-hour incubation with 2.5 μmol/L imatinib were increased in K562 cells (1.22 ± 0.11 *versus* 0.69 ± 0.07 μmol/g in the untreated control; $P = 0.009$) and CML-T1 cells (1.03 ± 0.07 *versus* 0.62 ± 0.19 μmol/g; $P = 0.01$). Glycerophosphocholine is an intermediate of membrane catabolism and a marker for membrane degradation processes. There were no significant changes in phospholipid synthesis/catabolism in HC-1 cells after imatinib treatment (Fig. 5*D*).

DISCUSSION

The discovery of the specific BCR-ABL tyrosine kinase inhibitor, imatinib (formerly STI571, Gleevec), has resulted in a new era of targeted cancer therapy. Due to its highly-specific mechanism of action, imatinib is well tolerated across a broad range of doses (1, 11, 12). One of the major concerns with imatinib treatment is the development of drug resistance of diverse origins in CML patients (13, 22). Recent clinical reports have indicated that changes in glucose metabolism might be related and/or predictive for the development of imatinib resistance. The control of glucose-substrate flux could be an important mechanism of the antiproliferative action of imatinib because BCR-ABL–positive cells express high-affinity GLUT-1 glucose transporter and demonstrate increased glucose uptake (14). Additionally, clinical studies of patients with imatinib-resistant c-KIT–positive tumors have demonstrated avid glucose uptake on PET scans (15). It has also been proposed that imatinib treatment may restrict *de novo* nucleic acid and fatty acid synthesis by inducing a significant fall in hexokinase and glucose-6-phosphate 1-dehydrogenase activities and altering pathway carbon flux of the pentose cycle (23). This could explain imatinib-induced inhibition of cell glucose substrate utilization and growth. However, significant aspects of the cel-

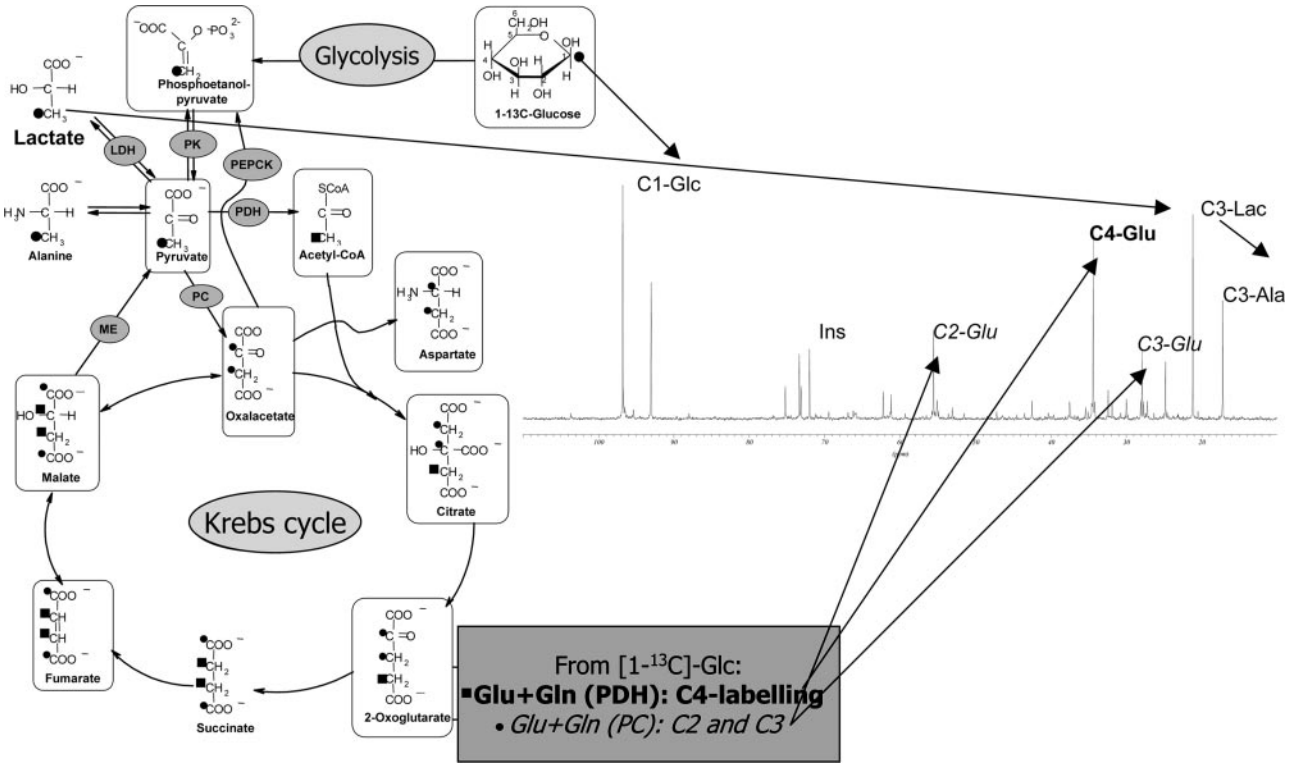

Fig. 6 Metabolic pathways of [1-^{13}C]glucose trough glycolysis and the mitochondrial Krebs cycle. *LDH,* C3-labeling in lactate; *PC,* C2 and C3 labeling in glutamate; *PDH,* C4 labeling in glutamate.

lular metabolic response (mitochondrial activity, energy production, membrane synthesis, and degradation) to imatinib treatment remain unknown, due to the lack of an appropriate assay that permits simultaneous observation of various biochemical pathways. In this study, we used MRS to assess changes in cell glucose metabolism in human BCR-ABL–positive cells after exposure to imatinib while also monitoring their vitality (energy charge NTP/NDP). We chose a concentration range of imatinib that encompasses concentrations above and below established IC_{50} values for K562 and CML-T1 cells. The IC_{50} values in our study correlated well with those reported previously in the literature (6, 12, 23).

Biochemistry of a tumor, especially glucose uptake and metabolism, is very different from that of the normal cell: mitochondrial metabolism is impaired; and cytosolic glycolysis is elevated (Warburg effect). This makes MRS one of the most valuable techniques to evaluate cancer metabolism and efficacy of the treatment because both glycolysis and the Krebs cycle can be assessed simultaneously. Incubation of cells with [1-^{13}C]glucose allows for metabolic transfer of C1-labeled glucose carbon to C3 pyruvate through glycolysis (Fig. 6). Then, pyruvate is quickly metabolized to the end product of cytosolic glycolysis, lactate. ^{13}C MRS allows for the detection of ^{13}C enrichment in C3-lactate from C3 pyruvate [through lactate dehydrogenase (LDH)]. On the other hand, pyruvate can enter the mitochondrial Krebs cycle in two different ways: directly through pyruvate dehydrogenase (PDH) or through pyruvate carboxylase [PC (anaplerotic way)]. In ^{13}C MR spectra, the C3 labeling of pyruvate will be seen in C4-glutamate (PDH activity) and/or C2-, C3-glutamate (PC activity; Fig. 6). Therefore, C3-lactate and C4-glutamate are markers for cytosolic glycolysis and the mitochondrial Krebs cycle, respectively.

Addition of low concentrations of imatinib strongly suppressed glycolitic activity (C3-lactate production from [1-^{13}C]glucose through glycolysis and LDH). Simultaneously, the increase in C4-glutamate production from [1-^{13}C]glucose (through PDH) indicated activation of the mitochondrial Krebs cycle by imatinib (at or below the IC_{50} values). The suppression of glycolysis and activation of the Krebs cycle resulted in decreased [1-^{13}C]glucose uptake from the incubation media. The most surprising finding of our study was that at therapeutically relevant concentrations, imatinib normalized energy state in BCR-ABL positive cells. This observation can only be partly explained by decreased energy utilization that results from inhibition of cell proliferation. Another explanation is that this increased energy production is a result of specific changes in glucose metabolism, *e.g.,* improvement/activation of the mitochondrial Krebs cycle. This suggests that imatinib-related stimulation of mitochondrial metabolism and reduction of anaerobic glycolysis in BCR-ABL–positive leukemia cells (reversed Warburg effect) resulted in higher energy state. The absence of apoptotic and/or necrotic cells at low imatinib concentrations correlated with the improvement in cell bioenergetics. The metabolic shift from glycolitic to mitochondrial oxidative metabolism was concomitant with inhibition of proliferation and may reflect cellular differentiation. At concentrations above 1

μmol/L, when the first signs of apoptosis were observed in K562 cells, the energy state and glutamate production dramatically decreased. The ”bell-shaped“ nature of the metabolic response enables a distinction between therapeutic effects at lower concentrations and typical signs of nonspecific cytotoxicity [seen, for example, with the standard antineoplastic therapies (18, 24, 25)] at higher concntrations.

The decreased concentrations of phosphocholine (PMEs), observed in this study are likely related to the inhibition of cell proliferation and cell differentiation processes. Phosphocholine, the major precursor for membrane synthesis, is known to be increased in all rapidly proliferating malignant cells including leukemia cells (26–28). An increase in glycerophoshocholine (PDEs), a membrane catabolism product, is related to apoptotic processes and membrane dysfunctions (18). At higher imatinib concentrations, apoptosis was observed in BCR-ABL–positive cells, and increased PDE concentrations were a metabolic marker for membrane degradation processes.

Finally, the increased concentration of Glc_e in the media of imatinib-treated cells correlated well with previous findings. The prior studies reported that imatinib regulates glucose flux through down-regulation of GLUT-1 transporters in human leukemia cells (14) and that glucose uptake is increased in imatinib-resistant tumors (15). Our results provide additional insight into the changes in glucose transport. Because imatinib exposure results in a greater metabolic activity of the Krebs cycle and less lactate production, glucose utilization via cytosolic glycolysis (Warburg effect) is reduced, resulting in diminished cellular requirement for glucose transport. Likewise, the increased uptake of 18-fluoro-2-deoxy-glucose, described in the clinical PET studies, could be a result of diminished mitochondrial activation in imatinib-resistant tumor cells. These findings may be important in the evaluation, prediction, and diagnosis of imatinib-resistant tumors and could lead to the earlier identification of patients who should receive alternative therapies. Whether imatinib interferes directly with mitochondrial enzymes or acts indirectly through tyrosine kinase inhibition is not yet known and has to be evaluated.

Since Warburg’s discovery, a great deal of research has provided information regarding mitochondrial metabolic dysfunction in cancer cells. It has been demonstrated that most tumor cells are characterized by diminished energy level and that the reduced metabolic state of the cell, as defined by a bioenergetic mitochondrial index relative to the cellular glycolitic potential, provides a signature of carcinogenesis (24). Most classic chemotherapeutic agents nonselectively decrease this already impaired energy production of cancer cells (18). Some novel anticancer agents have been shown to be highly effective in killing cancer cells through direct mitochondrial toxicity (29–32). In either case, the mechanism of drug action results in a decreased energy state and subsequent cell death. For the first time, we report normalization of cell bioenergetics and glucose metabolism by an antineoplastic agent that concurrently possesses high therapeutic efficacy (BCR-ABL activity inhibition). The novel signal transduction inhibitor imatinib inhibits cell proliferation in BCR-ABL–positive cells due to the inhibition of BCR-ABL tyrosine kinase activity. However, imatinib, unlike most existing anticancer agents, does not possess cytocidal activity at clinically relevant concentrations. Imatinib improves cell bioenergetics due to stimulation of mitochondrial glucose metabolism while inhibiting glycolitic activity. This unique regulatory metabolic activity of imatinib provides a novel signature for the efficacy of signal transduction therapy. MRS represents a novel metabolic approach for evaluation of drug efficacy that could be very useful in the development of novel anticancer agents, where therapeutic success is dependent on biological rather than toxicological effects.

ACKNOWLEDGMENTS

We thank Timo Dansauer (University of Bremen) and Lisa M. Frisch (University of Colorado Health Sciences Center) for technical support with the cell cultures. We thank Drs. Peter Marbach and Elisabeth Buchdunger (Novartis Pharma AG) for providing us with the study compound. Our special thanks go to Drs. Junia V. Melo (Imperial College, London, United Kingdom), Dieter Leibfritz (University of Bremen), and Claus U. Niemann (University of California, San Francisco, CA) for valuable suggestions and scientific discussions during manuscript preparation. We appreciate the help of Jamie Bendrick-Peart in stylistic corrections of the manuscript.

REFERENCES

1. O’Bryen SG, Guilhot F, Larson RA, et al. Imatinib compared with interferon and low-dose cytarabine for newly diagnosed chronic-phase chronic myeloid leukemia. N Engl J Med 2003;348:994–1004.

2. Peggs K, Mackinnon S. Imatinib mesylate: the new gold standard for treatment of chronic myeloid leukemia. N Engl J Med 2003;348: 1048–50.

3. Borgaonkar DS. Philadelphia-chromosome translocation and chronic myeloid leukemia. Lancet 1973;1:1250.

4. Hehlmann R, Hochhaus A, Berger U, Reiter A. Current trends in the management of chronic myelogenous leukemia. Ann Hematol 2000;79: 345–54.

5. Carlesso N, Griffin JD, Druker BJ. Use of a temperature-sensitive mutant to define the biological effects of the p210BCT-ABL tyrosine kinase on proliferation of a factor-dependent murine myeloid cell line. Oncogene 1994;9:149–56.

6. Deiniger MWN, Goldman JM, Lydon N, Melo JV. The tyrosine kinase inhibitor CGP57148B selectively inhibits the growth of BCR-ABL positive cells. Blood 1997;90:3691–8.

7. Vigneri P, Wang JY. Indication of apoptosis in chronic myelogenous leukemia cells through nuclear entrapment of BCR-ABL tyrosine kinase. Nat Med 2001;7:228–34.

8. Krystal GW, Honsawek S, Litz J, Buchdunger E. The selective tyrosine kinase inhibitor STI571 inhibits small cell lung growth. Clin Cancer Res 2000;6:3319–26.

9. Joensuu H. Treatment of inoperable gastrointestinal stromal tumor (GIST) with imatinib (Glivec, Gleevec). Med Klin 2002;97(Suppl 1): 28–30.

10. Tuveson DA, Willis NA, Jacks T, et al. STI571 inactivation of the gastrointestinal stromal tumor c-KIT oncoprotein: biological and clinical implications. Oncogene 2001;20:5054–8.

11. Druker BJ, Talpaz M, Resta DJ, et al. Efficacy and safety of a specific inhibitor of the BCR-ABL tyrosine kinase in chronic myeloid leukemia. N Engl J Med 2001;344:1031–7.

12. Kantarjian H, Sawyers C, Hochhaus A, et al. Hematologic and cytogenetic responses to imatinib mesylate in chronic myelogenous leukemia. N Engl J Med 2002;346:645–53.

13. Von Bubnoff N, Schneller F, Peschel C, Duyster J. BCR-ABL gene mutations in relation to clinical resistance of Philadelphia-chromosome-positive leukemia to STI571: a prospective study. Lancet 2002;359: 487–91.

14. Boros LG, Lee WN, Go VL. A metabolic hypothesis of cell growth and death in pancreatic cancer. Pancreas 2002;24:26–33.

15. Van den Abbeele AD, Balawi RD. Use of positron emission tomography (PET) in oncology and its potential role to assess response to imatinib mesylate therapy in gastrointestinal stromal tumors (GISTs). Eur J Cancer 2002;38:S60–5.

16. Leibfritz D. An introduction to the potential of ^{1}H-, ^{31}P- and ^{13}C-NMR spectroscopy. Anticancer Res 1996;16:1317–24.

17. Mountford CE, Doran S, Lean CL, Russell P. Cancer pathology in the year 2000. Biophys Chem 1997;68:127–35.

18. Evelhoch JL, Gillies RJ, Karczmar GS, et al. Applications of magnetic resonance in model systems: cancer therapeutics. Neoplasia 2000;2:152–65.

19. Serkova N, Brand A, Christians U, Leibfritz D. Evaluation of the effects of immunosuppressants on neuronal and glial cells in vitro by multinuclear magnetic resonance spectroscopy. Biochim Biophys Acta 1996;1314:93–104.

20. Serkova N, Jacobsen W, Niemann CU, et al. Sirolimus, but not the structurally related RAD (everolimus), enhances the negative effects of cyclosporine on mitochondrial metabolism in the rat brain. Br J Pharmacol 2001;133:875–85.

21. Kochi S, Takanaga H, Matsuo H, et al. Induction of apoptosis in mouse brain capillary endothelial cells by cyclosporin A and tacrolimus. Life Sci 2000;66:2255–60.

22. Hoover RR, Mahon FX, Melo JV, Daley GQ. Overcoming STI571 resistance with the farnesyl transferase inhibitors SCH66336. Blood 2002;100:1068–71.

23. Boren J, Cascante M, Marin S, et al. Gleevec (STI571) influences metabolic enzyme activities and glucose carbon flow toward nucleic acid and fatty acid synthesis in myeloid tumor cells. J Biol Chem 2001;276:37747–53.

24. Cuezva JM, Krajewska M, Lopez de Heredia M, et al. The bioenergetic signature of cancer: a marker of tumor progression. Cancer Res 2002;62:6674–81.

25. Bernes-Price SJ, Sant ME, Christopherson RI, Kuchel PW. ^{1}H and ^{31}P NMR and HPLC studies on muse L1210 leukemia cell extracts: the effect of Au(I) and Cu(I) diphosphine complexes on the cell metabolism. Magn Reson Med 1991;18:142–58.

26. Ackerstaff E, Pflug BR, Nelson JB, Bhujwala ZM. Detection of increased choline compounds with proton nuclear magnetic resonance spectroscopy to malignant transformation of human prostatic epithelial cells. Cancer Res 2001;61:3599–603.

27. Ackerstaff E, Glunde K, Bhujwalla ZM. Choline phospholipid metabolism: a target in cancer cells? J Cell Biochem 2003;90:525–33.

28. Franks SE, Smith MR, Aria-Mendoza F, et al. Phosphomonoester concentrations differ between chronic lymphocytic leukemia cells and normal human lymphocytes. Leukemia Res 2002;26:919–26.

29. Wosikowski K, Matter K, Schemainda I, et al. WK175, a novel antitumor agent, decreases the intracellular nicotinamide adenine dinucleotide concentration and induces the apoptotic cascade in human leukemic cells. Cancer Res 2002;2002:1057–62.

30. Holmuhamedov E, Lewis L, Bienengraeber M, et al. Suppression of human tumor cell proliferation trough mitochondrial targeting. FASEB J 2002;16:1010–6.

31. Geschwind JFH, Ko YH, Torbenson MS, Magee C, Pedersen PL. Novel therapy for liver cancer: direct intraarterial injection of a potent inhibitor of ATP production. Cancer Res 2002;62:3909–13.

32. Zhou R, Vander Heiden MG, Rudin CM. Genotoxic exposure is associated with alterations in glucose uptake and metabolism. Cancer Res 2002;62:3515–20.